PHILOSOPHICAL TRANSACTIONS OF THE ROYAL SOCIETY B

Phil. Trans. R. Soc. B (2008) **363**, 1179–1188
doi:10.1098/rstb.2007.2213
Published online 17 October 2007

Glutamate-354 of the CP43 polypeptide interacts with the oxygen-evolving Mn_4Ca cluster of photosystem II: a preliminary characterization of the Glu354Gln mutant

Melodie A. Strickler[1], Hong Jin Hwang[2], Robert L. Burnap[2], Junko Yano[3], Lee M. Walker[1], Rachel J. Service[1], R. David Britt[4], Warwick Hillier[5] and Richard J. Debus[1,*]

[1]*Department of Biochemistry, University of California, Riverside, CA 92521, USA*
[2]*Department of Microbiology and Molecular Genetics, Oklahoma State University, Stillwater, OK 74078, USA*
[3]*Physical Biosciences Division, Lawrence Berkeley National Laboratory, Berkeley, CA 94720, USA*
[4]*Department of Chemistry, University of California, Davis, CA 95616, USA*
[5]*Photobioenergetics Group, Research School of Biological Sciences, The Australian National University, Canberra, Australian Capital Territory 0200, Australia*

In the recent X-ray crystallographic structural models of photosystem II, Glu354 of the CP43 polypeptide is assigned as a ligand of the O_2-evolving Mn_4Ca cluster. In this communication, a preliminary characterization of the CP43-Glu354Gln mutant of the cyanobacterium *Synechocystis* sp. PCC 6803 is presented. The steady-state rate of O_2 evolution in the mutant cells is only approximately 20% compared with the wild-type, but the kinetics of O_2 release are essentially unchanged and the O_2-flash yields show normal period-four oscillations, albeit with lower overall intensity. Purified PSII particles exhibit an essentially normal S_2 state multiline electron paramagnetic resonance (EPR) signal, but exhibit a substantially altered S_2-*minus*-S_1 Fourier transform infrared (FTIR) difference spectrum. The intensities of the mutant EPR and FTIR difference spectra (above 75% compared with wild-type) are much greater than the O_2 signals and suggest that CP43-Glu354Gln PSII reaction centres are heterogeneous, with a minority fraction able to evolve O_2 with normal O_2 release kinetics and a majority fraction unable to advance beyond the S_2 or S_3 states. The S_2-*minus*-S_1 FTIR difference spectrum of CP43-Glu354Gln PSII particles is altered in both the symmetric and asymmetric carboxylate stretching regions, implying either that CP43-Glu354 is exquisitely sensitive to the increased charge that develops on the Mn_4Ca cluster during the $S_1 \rightarrow S_2$ transition or that the CP43-Glu354Gln mutation changes the distribution of Mn(III) and Mn(IV) oxidation states within the Mn_4Ca cluster in the S_1 and/or S_2 states.

Keywords: Fourier transform infrared spectroscopy (FTIR); Mn cluster; oxygen evolution; S-state cycle; water oxidation; site-directed mutagenesis

1. INTRODUCTION

The catalytic site of water oxidation in photosystem II (PSII) contains a cluster of four Mn ions and one Ca ion. The Mn ions accumulate oxidizing equivalents in response to light-induced electron transfer reactions within PSII and serve as the interface between one-electron photochemistry and the four-electron process of water oxidation (for reviews, see Goussias *et al.* (2002), Sauer & Yachandra (2004), Hillier & Messinger (2005) and McEvoy & Brudvig (2006)). During each catalytic cycle, the Mn_4Ca cluster cycles through five oxidation states termed S_n, where 'n' denotes the number of oxidizing equivalents that have been stored ($n=0$–4). The S_1 state predominates in dark-adapted samples. Most interpretations of Mn X-ray absorption near edge structure (XANES) data have concluded that the S_1 state consists of two Mn(III) and two Mn(IV) ions and that the S_2 state consists of one Mn(III) and three Mn(IV) ions (for review, see Sauer *et al.* (2005) and Yachandra (2005)).

The amino acid residues that ligate the Mn_4Ca cluster are provided mainly by the D1 polypeptide, one of the core subunits of PSII. One exception is Glu354 of the CP43 polypeptide.[1] In the current approximately 3.5 Å structural model (Ferreira *et al.* 2004), this residue is a bidentate ligand of a single Mn ion. In the current approximately 3.0 Å structural model (Loll *et al.* 2005), this residue bridges two Mn ions, including the Mn ion that is ligated (in this model) by the α-COO^- group of D1-Ala344. The differences between the two structural models are probably caused by differences in

* Author for correspondence (richard.debus@ucr.edu).

One contribution of 20 to a Discussion Meeting Issue 'Revealing how nature uses sunlight to split water'.

data quality, extent of radiation damage and approach to interpreting the electron density. A recent polarized X-ray absorption fine structure (EXAFS) study of PSII single crystals (conducted with X-ray doses below the thresholds that cause radiation-induced reduction of the cluster's Mn(III)/Mn(IV) ions) provides compelling evidence that the structure of the native Mn_4Ca cluster differs significantly from the structures that are depicted in the approximately 3.5 and approximately 3.0 Å structural models (Yano *et al.* 2006). This study confirms earlier XANES and EXAFS studies of PSII single crystals (Yano *et al.* 2005) and PSII membrane multilayers (Grabolle *et al.* 2006) that provided compelling evidence that the X-ray doses that were used to irradiate the PSII crystals in the crystallographic studies would have rapidly reduced the Mn_4Ca cluster's Mn(III/IV) ions to their fully reduced Mn(II) states and significantly perturbed the structure of the Mn_4Ca cluster by disrupting μ-oxo bridges and altering Mn–ligand interactions (Yano *et al.* 2005; Grabolle *et al.* 2006). Consequently, the ligation environment of the native Mn_4Ca cluster may differ in important respects from the ligation environments that are depicted in approximately 3.5 and approximately 3.0 Å structural models.

Fourier transform infrared (FTIR) difference spectroscopy is an extremely sensitive tool for characterizing dynamic structural changes that occur during an enzyme's catalytic cycle, such as changes in molecular interactions, protonation states, bonding (including changes in metal coordination and hydrogen bonding), bond strengths and protein backbone conformations (Mäntele 1996; Barth & Zscherp 2002; Barth 2007). PSII contains an extensive array of vibrational modes that undergo shifts in frequency during the individual S-state transitions. Many of these shifts produce strikingly large features in specific S_{n+1}-*minus*-S_n FTIR difference spectra, and many are clearly attributable to frequency shifts of carboxylate residues (for review, see Chu *et al.* (2001), Noguchi & Berthomieu (2005) and Noguchi (2007, in press)). The identification of these modes will complement X-ray crystallographic studies by providing information about the dynamic structural changes that accompany water oxidation and by helping to identify the specific Mn ion(s) that undergo oxidation during each S-state transition and the amino acid residues that facilitate the oxidation of Mn_4Ca cluster or that participate in proton transfer pathways leading from the Mn_4Ca cluster to the thylakoid lumen.

Attempts to identify specific modes in the FTIR difference spectra of PSII have focused on D1-Asp170 (Debus *et al.* 2005), D1-Glu189 (Kimura *et al.* 2005*b*; Strickler *et al.* 2006), D1-Asp342 (Strickler *et al.* 2007) and the α-COO^- group of D1-Ala344 (Chu *et al.* 2004; Mizusawa *et al.* 2004*a*,*b*; Kimura *et al.* 2005*c*; Strickler *et al.* 2005). On the basis of isotopic labelling conducted with L-[1-^{13}C]alanine, the symmetric carboxylate stretching ($\nu_{sym}(COO^-)$) mode of the α-COO^- group of D1-Ala344 was identified in the $S_{2\text{-}minus}$-S_1 FTIR difference spectrum of wild-type PSII particles (Chu *et al.* 2004; Kimura *et al.* 2005*c*; Strickler *et al.* 2005). The frequency of the $\nu_{sym}(COO^-)$ mode of D1-Ala344 in the S_1 state and its approximately 17 or approximately 36 cm^{-1} downshift in the S_2 state imply that this group is a unidentate ligand of a metal ion whose charge increases during the $S_1 \rightarrow S_2$ transition (Chu *et al.* 2004; Kimura *et al.* 2005*c*; Strickler *et al.* 2005). To determine whether the α-COO^- group of D1-Ala344 ligates Mn or Ca, wild-type cells of *Synechocystis* sp. PCC 6803 were propagated in the presence of both Sr and either [1−^{13}C]alanine or unlabelled alanine (Strickler *et al.* 2005). The substitution of Sr for Ca significantly alters several symmetric and asymmetric carboxylate stretching modes (Kimura *et al.* 2005*a*; Strickler *et al.* 2005; Suzuki *et al.* 2006), including some that may correspond to one or more metal ligands, but importantly does *not* alter the $\nu_{sym}(COO^-)$ mode of the α-COO^- group of D1-Ala344 (Strickler *et al.* 2005). Because it seems highly improbable that the structural perturbations of the Mn_4Ca cluster that are induced by substituting Sr for Ca (including the perturbation of multiple carboxylate groups) would not *also* alter the $\nu_{sym}(COO^-)$ mode of a carboxylate residue that directly coordinates the Ca ion, it was concluded that D1-Ala344 ligates Mn rather than Ca (Strickler *et al.* 2005).[2] The downshift of the $\nu_{sym}(COO^-)$ mode of D1-Ala344 that occurs during the $S_1 \rightarrow S_2$ transition is reversed during the $S_3 \rightarrow S_0$ transition (Kimura *et al.* 2005*c*; Debus in press).

Subsequent studies have shown that neither D1-Asp170 (Debus *et al.* 2005), nor D1-Glu189 (Strickler *et al.* 2006), nor D1-Asp342 (Strickler *et al.* 2007) is sensitive to the oxidation of the Mn_4Ca cluster during the $S_0 \rightarrow S_1$, $S_1 \rightarrow S_2$ or $S_2 \rightarrow S_3$ transitions. Two interpretations have been advanced to account for the insensitivity of these three amino acid residues to these three S-state transitions. One interpretation is that the increased charge that develops on the Mn_4Ca cluster during the $S_1 \rightarrow S_2$ transition is localized to the Mn ion that is coordinated by the α-COO^- group of D1-Ala344, and that any increase in charge that develops on the Mn_4Ca cluster during the $S_0 \rightarrow S_1$ and $S_2 \rightarrow S_3$ transitions is localized on the *one* Mn ion that is not ligated by D1-Asp170, D1-Glu189, D1-Asp342 or D1-Ala344 in either structural model (Strickler *et al.* 2006, 2007). In both structural models (Ferreira *et al.* 2004; Loll *et al.* 2005), this one Mn ion is ligated by Glu354 of the CP43 polypeptide. A second interpretation is that the carboxylate ligands of the Mn_4Ca cluster are mostly insensitive to changes in the formal oxidation states of the individual Mn ions (McEvoy *et al.* 2005; Sproviero *et al.* 2006). This situation might arise if the S-state transitions cause little increase in the electrostatic charge of the individual Mn ions, a prediction that was obtained from a QM/MM analysis of the approximately 3.5 Å X-ray crystallographic structural model (Sproviero *et al.* 2006). This situation might also arise if most of the Mn_4Ca cluster's Mn-ligating carboxylate ligands bind as equatorial ligands and the α-COO^- group of D1-Ala344 ligates along the Jahn–Teller axis of a Mn(III) ion. If so, then the approximately 16 or approximately 34 cm^{-1} downshift of this group's symmetric carboxylate stretching mode during the $S_1 \rightarrow S_2$ transition might arise from the shortening of the Mn–O bond that would occur when this Mn(III) ion is oxidized to its Mn(IV) oxidation state.[3]

To distinguish between these two explanations, we have begun a characterization of the mutants CP43-Glu354Gln and CP43-Glu354Asp. In this communication, we report a preliminary characterization of the CP43-Glu354Gln mutant. We find that CP43-Glu354 interacts with the Mn_4Ca cluster with sufficient strength so that either its carboxylate stretching modes are exquisitely sensitive to the $S_1 \rightarrow S_2$ transition or that the CP43-Glu354Gln mutation changes the distribution of Mn(III) and Mn(IV) oxidation states within the Mn_4Ca cluster in the S_1 and/or S_2 states.

2. MATERIAL AND METHODS

(a) *Construction of mutant and propagation of cultures*

The CP43-Glu354Gln mutation was constructed in the *psbC* gene of *Synechocystis* sp. PCC 6803 and transformed into a host strain of *Synechocystis* that lacks the large extrinsic loop of CP43 and contains a hexahistidine tag (His-tag) fused to the C-terminus of CP47 (the cloned *psbC* gene was the kind gift of W. F. J. Vermaas (Arizona State University)); our strategy for introducing mutations into the large extrinsic loop of CP43 is similar to that described by Goldfarb *et al.* (1997); the addition of a His-tag to CP47 has been described previously (Debus *et al.* 2001). The wild-type strain (WT-CP43) employed for the FTIR experiments of figure 4 was constructed in an identical manner as the CP43-Glu354Gln mutant strain except that the transforming plasmid carried no site-directed mutations. Single colonies were selected for ability to grow on solid media containing 5 μg ml^{-1} kanamycin monosulphate. Solid media contained 5 mM glucose and 10 μM DCMU. The DCMU and antibiotic were omitted from the liquid cultures. Large-scale liquid cultures (3×7 l) were propagated as described previously (Strickler *et al.* 2007). To verify the integrity of the mutant cultures that were harvested for the purification of thylakoid membranes and PSII particles, an aliquot of each culture was set aside and the sequence of the portion of the *psbC* gene that encodes the large extrinsic loop of CP43 was obtained after PCR amplification of genomic DNA (Chu *et al.* 1994). No trace of the wild-type codon was detected in any of the mutant cultures.

(b) *Purification of thylakoid membranes*

Thylakoid membranes were isolated under dim green light at 4°C following the procedure of Tang & Diner (1994), as modified by Strickler *et al.* (2005). Harvested cells were concentrated and suspended in a buffer containing 1.2 M betaine, 10% (v/v) glycerol, 50 mM MES–NaOH (pH 6.0), 5 mM $CaCl_2$, 5 mM $MgCl_2$, 1 mM benzamidine, 1 mM ε-amino-*n*-caproic acid, 1 mM phenylmethylsulphonyl fluoride and 0.05 mg ml^{-1} DNase I, and then broken by nine cycles of (5 s on/15 min off) in a glass bead homogenizer (Bead-Beater, BioSpec Products, Bartlesville, OK). After separation of unbroken cells and debris by centrifugation, the resulting thylakoid membranes were concentrated by centrifugation (20 min at 40 000*g* in a Beckman Ti45 rotor) and suspended to a concentration of 1.0–1.5 mg of Chl ml^{-1} in a buffer containing 1.2 M betaine, 10% (v/v) glycerol, 50 mM MES–NaOH (pH 6.0), 20 mM $CaCl_2$ and 5 mM $MgCl_2$. The concentrated thylakoid membranes were either flash-frozen as 1 ml aliquots in liquid nitrogen and stored at −80°C, or used immediately for the purification of PSII particles.

(c) *Purification of PSII particles*

Isolated PSII particles were purified under dim green light at 4°C with Ni-NTA superflow affinity resin (Qiagen, Valentia, CA) as described previously (Strickler *et al.* 2005). The purification buffer consisted of 1.2 M betaine, 10% (v/v) glycerol, 50 mM MES–NaOH (pH 6.0), 20 mM $CaCl_2$, 5 mM $MgCl_2$, 50 mM histidine, 1 mM EDTA and 0.03% (w/v) *n*-dodecyl β-D-maltoside. The purified PSII particles were concentrated to approximately 1.0 mg of Chl ml^{-1} by ultrafiltration, frozen in liquid N_2 and stored at −196°C (vapour phase nitrogen).

(d) *Flash O_2 yield and kinetic measurements*

Measurements were performed with a bare platinum electrode that permits the centrifugal deposition of samples onto the electrode surface (Burnap *et al.* 1996). Thylakoid membranes were concentrated by centrifugation and suspended at approximately 0.8 mg of Chl ml^{-1} in 50 mM HEPES–NaOH (pH 7.2), 5 mM $CaCl_2$, 10 mM $MgCl_2$ and 1 M sucrose (Qian *et al.* 1999). For each measurement, 3.2 μg of Chl were centrifugally deposited at 18 000*g* for 10 min onto the platinum surface of the electrode in a Sorvall HB-4 swing-out rotor. Samples were dark adapted for 10 min prior to the initiation of the flash sequence. Polarization of the electrode (0.73 V) was initiated 10 s before the initiation of data acquisition and the flash sequence (15 flashes at a frequency of 4 Hz) was initiated 333 ms after that. Analysis of S-state parameters was performed according to Lavorel (1976) and Meunier *et al.* (1995).

(e) *Electron paramagnetic resonance(EPR) measurements*

Continuous-wave EPR spectra were recorded with a Varian E-109 system, a standard TE102 cavity and a Heli-tran liquid helium cryostat (Air Products, Allentown, PA). Sample manipulations were conducted under dim green light at 4°C. The samples were concentrated to 9–11 mg of Chl ml^{-1} with Centricon-100 concentrators (Millipore Corp., Bedford, MA), transferred to Mylar sample holders, extensively dark adapted, and then frozen in liquid nitrogen. The S_2 state was generated by illuminating samples for 5 min in a non-silvered Dewar at 198 K (dry ice/ethanol) with a focused, heat-filtered, 350 W Radiac light source. The samples were then immediately frozen in liquid nitrogen.

(f) *Preparation of FTIR samples*

All manipulations were conducted under dim green light at 4°C. Samples were exchanged into FTIR analysis buffer (40 mM sucrose, 10 mM MES–NaOH (pH 6.0), 5 mM $CaCl_2$, 5 mM NaCl and 0.06% (w/v) *n*-dodecyl β-D-maltoside; Yamanari *et al.* 2004; Debus *et al.* 2005) by passage through a centrifugal gel filtration column (Strickler *et al.* 2006). Concentrated samples (approx. 10 μl in volume) were mixed with 1/10 volume of fresh 100 mM potassium ferricyanide (dissolved in water), spread to a diameter of approximately 10 mm on a 15 mm diameter BaF_2 window, and then dried lightly (until tacky) under a stream of dry nitrogen gas. To maintain the humidity of the sample in the FTIR cryostat at 99% RH, 1 μl of 20% (v/v) glycerol (in water) was spotted onto the window, adjacent to the sample, but not touching it (Noguchi & Sugiura 2002). A second IR window with a Teflon spacer (0.5 mm thick) was placed over the first and sealed in place with silicon-free high-vacuum grease. The sample was loaded immediately into the FTIR cryostat at 273.0 K and allowed to equilibrate in darkness for 2 hours. Sample concentrations and thicknesses

were adjusted so that the absolute absorbance of the amide I band at 1657 cm^{-1} was 0.7–1.1.

(**g**) ***Measurement of FTIR spectra***

Mid-frequency FTIR spectra were recorded with a Bruker Equinox 55 spectrometer (Bruker Optics, Billerica, MA) at a spectral resolution of 4 cm^{-1} as described previously (Debus *et al.* 2005; Strickler *et al.* 2006, 2007). Flash illumination (approx. 20 mJ per flash, approx. 7 ns fwhm) was provided by a frequency-doubled Q-switched Nd:YAG laser (Surelite I; Continuum, Santa Clara, CA). After dark adaptation, one pre-flash was applied followed by 5 min of additional dark adaptation. This treatment was employed to oxidize Y_D and to maximize the proportion of centres in the S_1 state. Six successive flashes were then applied with an interval of 12.2 s between each. Two single-beam spectra were recorded before the first flash and one single-beam spectrum was recorded starting at 0.33 s after the first and subsequent flashes (each single-beam spectrum consisted of 100 scans). The 0.33 s delay was incorporated to allow for the oxidation of $Q_A^{\bullet-}$ by the ferricyanide. The difference spectra corresponding to the $S_1 \rightarrow S_2$ transition was obtained by dividing the single-beam spectrum that was recorded after the first flash by the single-beam spectrum that was recorded immediately before the first flash and the ratio was converted to units of absorption. The sample was dark adapted for 30 min and then the entire cycle was repeated, including the pre-flash and the 5 min additional dark-adaptation period. The entire cycle was repeated 12 times for each wild-type sample and 4–10 times for each CP43-Glu354Gln sample. To improve the signal-to-noise ratio, the difference spectra recorded with multiple samples were averaged.

(**h**) ***Other procedures***

Chlorophyll concentrations and light-saturated steady-state rates of O_2 evolution were measured as described previously (Chu *et al.* 2004).

3. RESULTS

The light-saturated, steady-state O_2-evolving activity of CP43-Glu354Gln cells was 90–100 μmol O_2 (mg of Chl)$^{-1}$ h^{-1} compared with 480–500 μmol O_2 (μg of Chl)$^{-1}$ h^{-1} for wild-type cells. The lower rate in mutant cells (18–21% compared with wild-type) is consistent with an earlier report (Rosenberg *et al.* 1999). The light-saturated O_2-evolving activity of purified CP43-Glu354Gln PSII particles was 0.52–0.97 mmol O_2 (mg of Chl)$^{-1}$ h^{-1} compared with 5.1–5.5 mmol O_2 (mg of Chl)$^{-1}$ h^{-1} for wild-type PSII particles. The lower activity of the purified PSII particles (10–18% compared with wild-type) suggests that the Mn_4Ca cluster in the CP43-Glu354Gln mutant may be somewhat labile.

The O_2 yield that is produced by each of a series of saturating single-turnover flashes provides a measure of the efficiency of the individual S-state transitions in samples that evolve O_2. The pattern of O_2-flash yields in CP43-Glu354Gln thylakoid membranes (figure 1) shows the same period-four oscillations that are observed in wild-type membranes, although the amplitudes are much smaller, consistent with the lower steady-state rates of O_2 evolution observed in the mutant cells and PSII particles. Our initial analysis of these data indicates that the miss factor (α) and dark distribution of S states are virtually the same in the mutant as in the wild-type control. The kinetics of O_2 release in CP43-Glu354Gln thylakoid membranes in comparison with wild-type is presented in figure 2. Our initial analysis of these data shows that the kinetics of O_2 release are virtually the same in the mutant as in the wild-type control.

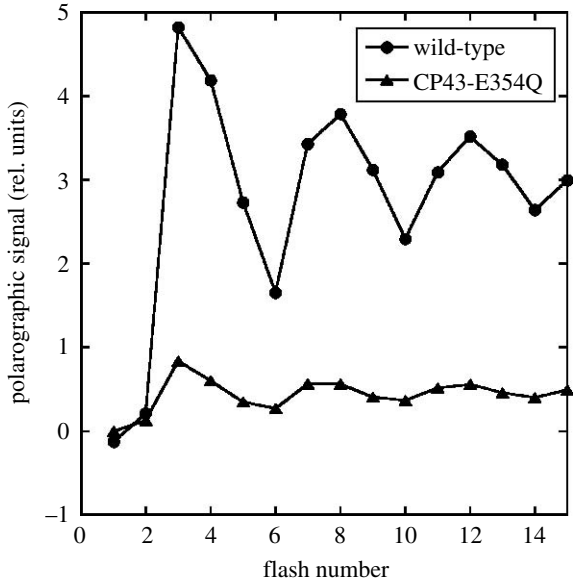

Figure 1. Comparison of the flash O_2 yield patterns of wild-type (circles) and CP43-Glu354Gln (triangles) thylakoid membranes in response to 15 saturating xenon flashes applied at a frequency of 4 Hz. Equivalent amounts of thylakoid membranes were deposited centrifugally on the surface of a bare platinum electrode and dark adapted for 10 min before the sequence of saturating flashes was initiated.

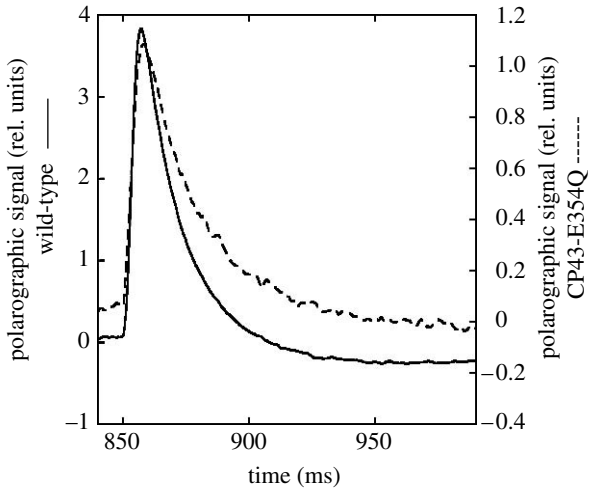

Figure 2. Comparison of the flash-induced O_2 signals of wild-type (solid line) and CP43-Glu354Gln (dashed line) thylakoid membranes. The traces have been normalized to facilitate comparison (the individual scales of the polarographic signals of the wild-type and CP43-Glu354Gln samples are given on the left and right axes, respectively). Equivalent amounts of thylakoid membranes were deposited centrifugally on the surface of a bare platinum electrode and given a sequence of 100 saturating xenon flashes at 4 Hz. The data show the averages from each set of 100 kinetic traces.

Light-*minus*-dark S_2 state multiline EPR spectra of CP43-Glu354Gln and wild-type PSII particles are compared in figure 3. The hyperfine splittings of the wild-type and mutant spectra are similar. The amplitudes of the spectra are roughly similar, although

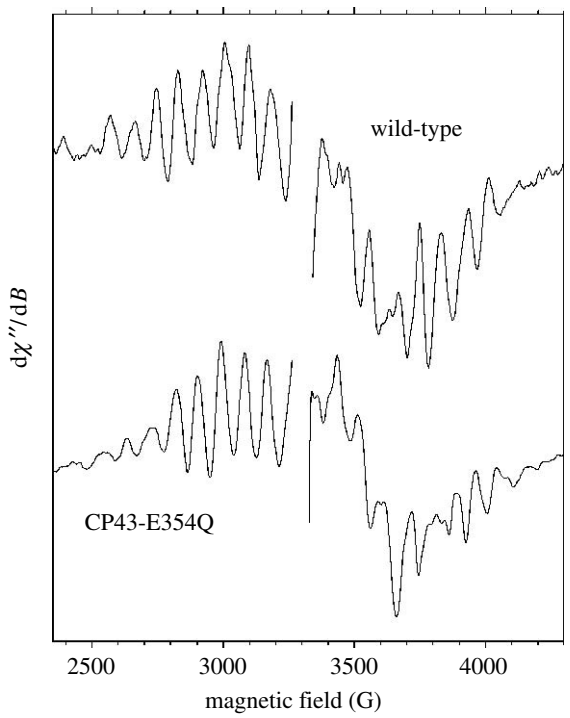

Figure 3. Comparison of the light-*minus*-dark S_2 multiline EPR signals in the wild-type (upper trace) and CP43-Glu354Gln (lower trace) PSII particles. The wild-type and mutant samples contained 9–11 mg of Chl ml^{-1} in 1.2 M betaine, 10% (v/v) glycerol, 10 mM MES–NaOH (pH 6.0), 10 mM $CaCl_2$, 5 mM $MgCl_2$, 50 mM histidine, 1 mM EDTA and 0.03% (w/v) *n*-dodecyl β-D-maltoside. The experimental conditions used were as follows: microwave frequency of 9.2444 GHz; microwave power of 30 mW; modulation amplitude of 32 G; modulation frequency of 100 kHz; time constant of 0.25 s; scan time of 4 min (3300 ± 2000 G scan range); and temperature of 8 K. To generate the S_2 state, the samples were illuminated for 5 min at 195 K before being flash-frozen in liquid nitrogen. Both spectra have had the large signal of $Y_D^{\bullet}$ at $g=2$ excised for clarity. Each spectrum represents the accumulation of five scans.

uncertainty in the Chl concentrations of the concentrated EPR samples precluded accurate quantitation.

The mid-frequency S_2-*minus*-S_1 FTIR difference spectra of CP43-Glu354Gln and wild-type PSII particles are compared in figure 4.[4] When the amplitudes of the spectra are normalized to the extent of flash-induced charge separation (accomplished by normalizing the mutant and wild-type spectra to the peak-to-peak amplitudes of the negative ferricyanide peak at 2115 cm^{-1} and the positive ferrocyanide peak at 2038 cm^{-1}), the amplitude of the S_2-*minus*-S_1 FTIR difference spectrum in the mutant was found to be approximately 75% of that of the wild-type, consistent with the approximately similar amplitudes of the light-induced S_2 state multiline EPR signals in the mutant and wild-type PSII particles. Therefore, to facilitate comparison of the mutant and wild-type spectra in figure 4, the amplitude of the mutant spectrum was multiplied by a factor of 1.3. Although numerous features in the mutant spectrum resemble those in the wild-type, the mutant spectrum differs significantly from that of the wild-type in both the asymmetric carboxylate stretching ($\nu_{asym}(COO^-)$) region and the symmetric carboxylate stretching ($\nu_{sym}(COO^-)$) region (the former region overlaps with the amide I and amide II regions). To isolate the altered modes and display them more clearly, the wild-type-*minus*-mutant double-difference spectrum is presented in figure 4 (lower trace). The main features in this spectrum are positive peaks at 1588, 1505, 1429, 1362 and 1334 cm^{-1}, and negative peaks at 1677, 1665, 1656, 1640, 1556, 1542, 1520, 1378 and 1351 cm^{-1}. These data show that one or more $\nu_{sym}(COO^-)$ and $\nu_{asym}(COO^-)$ modes may be absent or shifted in the mutant PSII particles. However, the large number of features in the amide I and amide II regions of the double-difference spectrum indicates that the CP43-Glu354Gln mutation may also perturb the polypeptide backbone in the vicinity of the Mn_4Ca cluster to a much larger extent than other mutations, such as D1-Asp170His (Debus *et al.* 2005), D1-Glu189Gln (Kimura *et al.* 2005*b*; Strickler *et al.* 2006), D1-Glu189Arg (Strickler *et al.* 2006), D1-Asp342Asn (Strickler *et al.* 2007) or D1-Ala344Gly (Chu *et al.* 2004; Mizusawa *et al.* 2004*a*,*b*).

4. DISCUSSION

Our observation that CP43-Glu354Gln thylakoid membranes exhibit normal O_2-release kinetics and normal period-four oscillations of O_2-flash yields shows that, in at least a fraction of CP43-Glu354Gln PSII reaction centres, the S-state transitions are not blocked. The diminished O_2 yield after each flash correlates with the overall lower steady-state O_2-evolving activity of CP43-Glu354Gln cells. On the basis of the relative amplitudes of the wild-type and mutant S_2-*minus*-S_1 FTIR difference spectra, we estimate that approximately 75% of the purified CP43-Glu354Gln PSII particles contain Mn_4Ca clusters. This estimate is consistent with our EPR data. Although we were unable to accurately quantify the amplitudes of the S_2 state multiline EPR spectra, the approximately similar amplitudes of this spectrum in the wild-type and mutant samples imply that most of CP43-Glu354Gln PSII particles contain assembled Mn_4Ca clusters. Because the intensities of the mutant EPR and FTIR difference spectra are much larger compared with wild-type than the amplitudes of the O_2-flash yields, we conclude that the CP43-Glu354Gln PSII reaction centres that contain Mn_4Ca clusters are heterogeneous, with a minority fraction able to evolve O_2 with normal O_2-release kinetics and a majority fraction capable of exhibiting S_2 state EPR and FTIR spectra, but unable to advance beyond the S_2 or S_3 states.

Unlike previously examined mutations constructed at D1-Asp170, D1-Glu189, D1-Asp342 and D1-Ala344, the CP43-Glu354Gln mutation causes substantial alterations in both the $\nu_{asym}(COO^-)$ and $\nu_{sym}(COO^-)$ regions of the S_2-*minus*-S_1 FTIR difference spectrum. One of the most dramatic alterations is the complete elimination of the 1588(+) cm^{-1} band. This band has been assigned (Noguchi *et al.* 1995; Taguchi & Noguchi 2007) to the $\nu_{asym}(COO^-)$ mode of a carboxylate residue that bridges between Mn and Ca or between two Mn ions (but see below). Because the $\nu_{asym}(COO^-)$ region overlaps the amide I and amide II regions, some of the observed spectral alterations in the $\nu_{asym}(COO^-)$

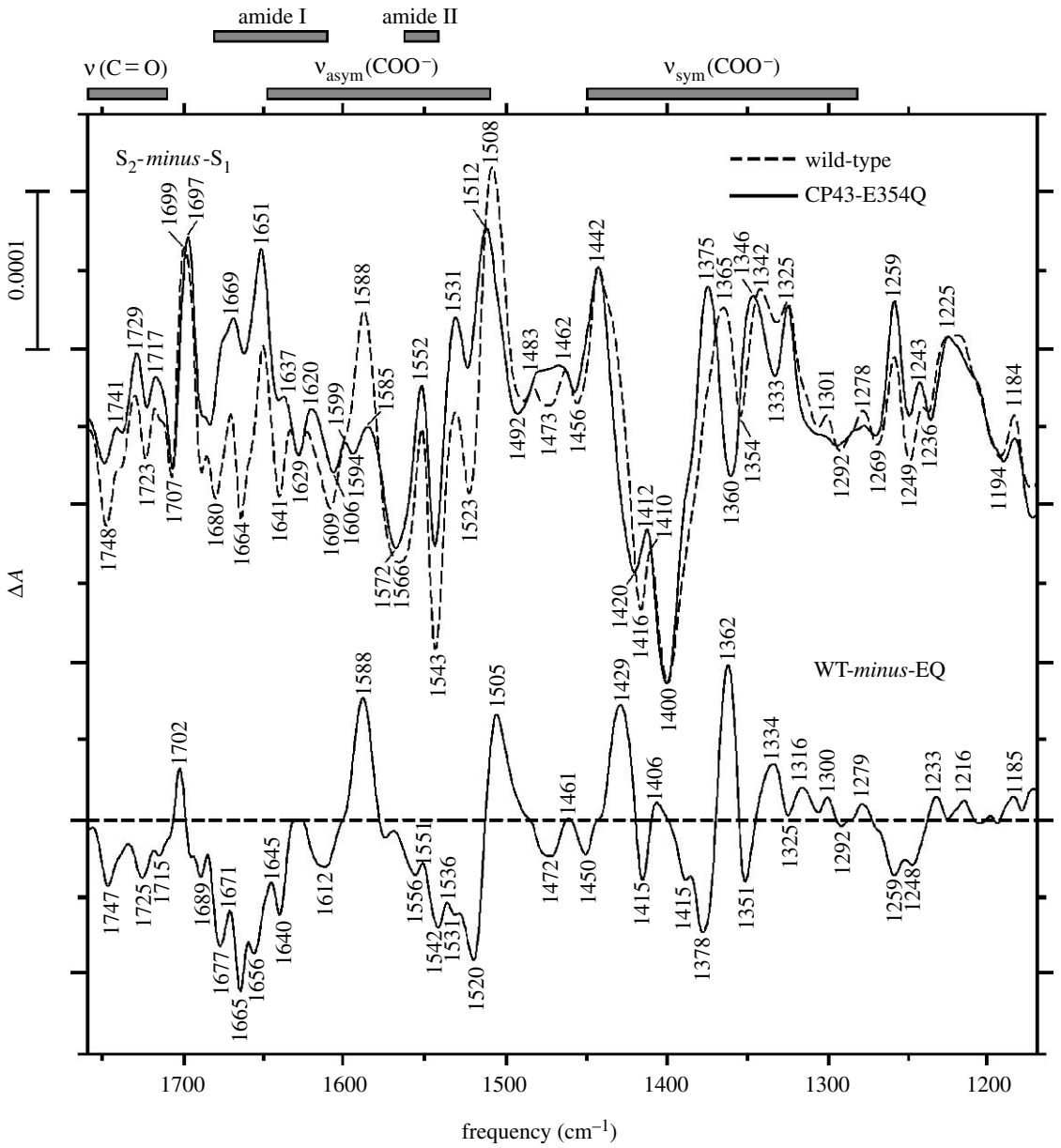

Figure 4. Comparison of the mid-frequency S_2-*minus*-S_1 FTIR difference spectra (upper traces) of CP43-Glu354Gln (solid lines) and WT-CP43 (dashed lines) PSII particles. The wild-type spectrum represents the average of 10 800 scans. The CP43-Glu354Gln spectrum represents the average of 31 500 scans. To facilitate comparison, the CP43-Glu354Gln spectrum was multiplied vertically by a factor of 1.3 after normalization of the wild-type and mutant spectra to the peak-to-peak amplitudes of the negative ferricyanide peak at 2115 cm^{-1} and the positive ferrocyanide peak at 2038 cm^{-1}. A wild-type-*minus*-mutant double-difference spectrum (lower trace) was calculated by directly subtracting the S_2-*minus*-S_1 FTIR difference spectra shown in the upper traces. The horizontal dashed line indicates the zero level.

region undoubtedly arise from mutation-induced perturbations to the polypeptide backbone. Amide II and $\nu_{asym}(COO^-)$ modes can be distinguished by their different sensitivities to the incorporation of ^{15}N: amide II modes are downshifted by 14–16 cm^{-1} whereas $\nu_{asym}(COO^-)$ modes are not shifted. Preliminary global ^{15}N-labelling experiments conducted with both wild-type and CP43-Glu354Gln PSII particles (M.A. Strickler *et al.* unpublished data) indicate that the 1588(+) cm^{-1} band and features near 1556(−) and 1530(−) cm^{-1} correspond to $\nu_{asym}(COO^-)$ modes. The assignment of the 1588(+) cm^{-1} feature to a $\nu_{asym}(COO^-)$ mode is consistent with earlier global ^{15}N-labelling studies (Noguchi *et al.* 1995; Noguchi & Sugiura 2003; Kimura *et al.* 2003; Yamanari *et al.* 2004). One possibility is that the 1588(+) and 1531(−) cm^{-1} features in the double-difference spectrum correspond to the $\nu_{asym}(COO^-)$ mode of CP43-Glu354 in the S_2 and S_1 states, respectively, and that the 1362(+) and 1378(−) cm^{-1} features correspond to the $\nu_{sym}(COO^-)$ mode of CP43-Glu354 in the S_2 and S_1 states, respectively. If so, then the frequency difference between the $\nu_{asym}(COO^-)$ and $\nu_{sym}(COO^-)$ modes would increase from approximately 153 cm^{-1} in the S_1 state to approximately 226 cm^{-1} in the S_2 state. Such an increase would be compatible with CP43-Glu354 ligating the Mn_4Ca cluster and changing its coordination mode during the $S_1 \rightarrow S_2$ transition from a bridging ligand between

two metal ions in the S_1 state to a unidentate ligand of a single metal ion in the S_2 state (Deacon & Phillips 1980; Nara *et al.* 1996; Nakamoto 1997).

However, the large number of features in the $\nu_{sym}(COO^-)$ region of the double-difference spectrum precludes a definite assignment of specific features to CP43-Glu354 at this time. Other interpretations are possible. For example, the structural perturbations introduced by the CP43-Glu354Gln mutation are sufficient to alter numerous amide I and amide II bands. These structural perturbations and/or the loss of the charge of CP43-Glu354 may be sufficient to change the Mn oxidation sequence such that an entirely different Mn ion undergoes oxidation during the $S_1 \rightarrow S_2$ transition in mutant and wild-type PSII centres. Indeed, preliminary experiments conducted with [1−^{13}C]alanine (M.A. Strickler *et al.* unpublished data) suggest that the Mn ion that is ligated by the α-COO^- group of D1-Ala344 does not undergo oxidation during the $S_1 \rightarrow S_2$ transition in CP43-Glu354Gln PSII particles. The 1351(−) and 1334(+) cm^{-1} features in the double-difference spectrum of figure 4 may reflect the insensitivity of D1-Ala344 to the Mn oxidation that occurs during the $S_1 \rightarrow S_2$ transition in this mutant. If the CP43-Glu354Gln mutation induces a different Mn ion to undergo oxidation during the $S_1 \rightarrow S_2$ transition, then many of the features that differ between the wild-type and mutant S_2-*minus*-S_1 FTIR difference spectra could reflect a difference in the distribution of Mn(III) and Mn(IV) oxidation states within the Mn_4Ca cluster in the S_1 and/or S_2 states. Consequently, without the examination of additional mutants, we cannot exclude the possibility that features in the double-difference spectrum, such as the 1588(+) cm^{-1} band, correspond to the $\nu_{asym}(COO^-)$ or $\nu_{asym}(COO^-)$ modes of carboxylate groups other than CP43-Glu354. Nevertheless, we *can* conclude that CP43-Glu354 interacts with the Mn_4Ca cluster with sufficient strength that either its $\nu_{asym}(COO^-)$ or $\nu_{asym}(COO^-)$ modes are present in the S_2-*minus*-S_1 FTIR difference spectrum of wild-type PSII particles (and are absent in the mutant PSII particles) or that the CP43-Glu354Gln mutation induces a redox isomerization of the Mn ions of the Mn_4Ca cluster.

One aspect of the mutant S_2-*minus*-S_1 FTIR difference spectrum is clear: the large positive feature at 1588 cm^{-1} is eliminated, yet the negative feature at 1400 cm^{-1} is unchanged. This observation is difficult to reconcile with an assignment of these two modes to a single Mn–Mn or Mn–Ca bridging carboxylate group that has its $\nu_{asym}(COO^-)$ mode at approximately 1587 cm^{-1} in the S_2 state and its $\nu_{sym}(COO^-)$ mode at approximately 1403 cm^{-1} in the S_1 state. This assignment has been proposed on the basis of analyses of Ca-depleted PSII preparations (Noguchi *et al.* 1995; Taguchi & Noguchi 2007). However, the S_2-*minus*-S_1 FTIR difference spectrum is altered far more substantially by Ca depletion than by the CP43-Glu354Gln mutation. We propose that substantially more amino acid residues in the environment of the Mn_4Ca cluster are perturbed by the depletion of Ca than by the substitution of CP43-Glu354 by Gln and that the 1588(+) and 1400(−) cm^{-1} features in the S_2-*minus*-S_1 FTIR difference spectrum of wild-type PSII particles correspond to different carboxylate groups.

This work was funded by the National Institutes of Health (GM-076232 and GM-066136 to R.J.D., GM-048242 to R.D.B. and GM-055302 to J.Y.), the National Science Foundation (MCB-0448567 to R.L.B.), the Australian Research Council (DP0770149 to W.H.) and the Department of Energy, Director, Office of Science, Office of Basic Energy Sciences, Chemical Sciences, Geosciences, and Biosciences Division (Contract DE-AC02-05CH11231 to J.Y.). The authors wish to thank Anh P. Nguyen for maintaining the mutant and wild-type cultures of *Synechocystis* sp. PCC 6803 and for purifying the thylakoid membranes that were used for measurements or for the isolation of PSII particles and V. S. Batista, G. W. Brudvig, V. L. Pecoraro and T. Noguchi for stimulating discussions about interpretations of past and present FTIR data.

ENDNOTES

[1]Multiple numbering systems are in use for CP43 (Bricker & Frankel 2002). The different numbering systems arise because (i) *psbC* (the gene encoding CP43) has an unusual start codon, (ii) CP43 is post-translationally processed at its amino terminus, and (iii) in *Synechocystis* sp. PCC 6803, there is a deletion of one residue at position 7 compared with the amino acid sequences of CP43 in other organisms. The numbering system used in this study is the same as that used in the X-ray crystallographic studies.

[2]It should be noted that some authors continue to assert that the α-COO^-group of D1-Ala344 ligates Ca rather than Mn (McEvoy & Brudvig 2006; Sproviero *et al.* 2006).

[3]This particular explanation was first suggested to us by Gary W. Brudvig.

[4]No significant differences were detected between data obtained with WT-CP43 and other wild-type control strains of *Synechocystis* 6803, such as those described in Strickler *et al.* 2006.

REFERENCES

Barth, A. 2007 Infrared spectroscopy of proteins. *Biochim. Biophys. Acta* **1767**, 1073–1101. (doi:10.1016/j.bbabio.2007.06.004)

Barth, A. & Zscherp, C. 2002 What vibrations tell us about proteins. *Q. Rev. Biophys.* **35**, 369–430. (doi:10.1017/S0033583502003815)

Bricker, T. M. & Frankel, L. K. 2002 The structure and function of CP47 and CP43 in photosystem II. *Photosynth. Res.* **72**, 131–146. (doi:10.1023/A:1016128715865)

Burnap, R. L., Qian, M. & Pierce, C. 1996 The manganese-stabilizing protein of photosystem II modifies the *in vivo* deactivation kinetics of the H_2O oxidation complex in *Synechocystis* sp, PCC 6803. *Biochemistry* **35**, 874–882. (doi:10.1021/bi951964j)

Chu, H.-A., Nguyen, A. P. & Debus, R. J. 1994 Site-directed photosystem ii mutants with perturbed oxygen evolving properties: 1. Instability or inefficient assembly of the manganese cluster *in vivo*. *Biochemistry* **33**, 6137–6149. (doi:10.1021/bi00186a013)

Chu, H.-A., Hillier, W., Law, N. A. & Babcock, G. T. 2001 Vibrational spectroscopy of the oxygen-evolving complex and of manganese model compounds. *Biochim. Biophys. Acta* **1503**, 69–82. (doi:10.1016/S0005-2728(00)00216-4)

Chu, H.-A., Hillier, W. & Debus, R. J. 2004 Evidence that the C-terminus of the D1 polypeptide is ligated to the manganese ion that undergoes oxidation during the S_1 to S_2 transition: an isotope-edited FTIR study. *Biochemistry* **43**, 3152–3166. (doi:10.1021/bi035915f)

Deacon, G. B. & Phillips, R. J. 1980 Relationships between the carbon–oxygen stretching frequencies of carboxylato complexes and the type of carboxylate coordination. *Coord. Chem. Rev.* **33**, 227–250. (doi:10.1016/S0010-8545(00)80455-5)

Debus, R. J. In press. Protein ligation of the photosynthetic oxygen-evolving center. *Coord. Chem. Rev.*

Debus, R. J., Campbell, K. A., Gregor, W., Li, Z.-L., Burnap, R. L. & Britt, R. D. 2001 Does histidine 332 of the D1 polypeptide ligate the manganese cluster in photosystem II? An electron spin echo envelope modulation study. *Biochemistry* **40**, 3690–3699. (doi:10.1021/bi002394c)

Debus, R. J., Strickler, M. A., Walker, L. M. & Hillier, W. 2005 No evidence from FTIR difference spectroscopy that aspartate-170 of the D1 polypeptide ligates a manganese ion that undergoes oxidation during the S_0 to S_1, S_1 to S_2, or S_2 to S_3 transitions in photosystem II. *Biochemistry* **44**, 1367–1374. (doi:10.1021/bi047558u)

Ferreira, K. N., Iverson, T. M., Maghlaoui, K., Barber, J. & Iwata, S. 2004 Architecture of the photosynthetic oxygen-evolving center. *Science* **303**, 1831–1838. (doi:10.1126/science.1093087)

Goldfarb, N., Knoepfle, N. & Putnam-Evans, C. 1997 Contruction of a *psbC* deletion strain in *Synechocystis* 6803. *SAAS Bull. Biochem. Biotechnol.* **10**, 1–6.

Goussias, C., Boussac, A. & Rutherford, A. W. 2002 Photosystem II and photosynthetic oxidation of water: an overview. *Phil. Trans. R. Soc. B* **357**, 1369–1381. (doi:10.1098/rstb.2002.1134)

Grabolle, M., Haumann, M., Müller, C., Liebisch, P. & Dau, H. 2006 Rapid loss of structural motifs in the manganese complex of oxygenic photosynthesis by X-ray irradiation at 10–300 K. *J. Biol. Chem.* **281**, 4580–4588. (doi:10.1074/jbc.M509724200)

Hillier, W. & Messinger, J. 2005 Mechanism of photosynthetic oxygen production. In *Photosystem II: the light-driven water: plastoquinone oxidoreductase* (eds T. Wydrzynski & Ki. Satoh), pp. 567–608. Dordrecht, The Netherlands: Springer.

Kimura, Y., Mizusawa, N., Ishii, A., Yamanari, T. & Ono, T.-A. 2003 Changes of low-frequency vibrational modes induced by universal ^{15}N- and ^{13}C-isotope labeling in S_2/S_1 FTIR difference spectrum of oxygen-evolving complex. *Biochemistry* **42**, 13 170–13 177. (doi:10.1021/bi035420q)

Kimura, Y., Hasegawa, K., Yamanari, T. & Ono, T.-A. 2005*a* Studies on photosynthetic oxygen-evolving complex by means of Fourier transform infrared spectroscopy: calcium and chloride cofactors. *Photosynth. Res.* **84**, 245–250. (doi:10.1007/s11120-005-0412-z)

Kimura, Y., Mizusawa, N., Ishii, A., Nakazawa, S. & Ono, T.-A. 2005*b* Changes in structural and functional properties of oxygen-evolving complex induced by replacement of D1-glutamate 189 with glutamine in photosystem II: ligation of glutamate 189 carboxylate to the manganese cluster. *J. Biol. Chem.* **280**, 37 895–37 900. (doi:10.1074/jbc.M505887200)

Kimura, Y., Mizusawa, N., Yamanari, T., Ishii, A. & Ono, T.-A. 2005*c* Structural changes of D1 C-terminal α-carboxylate during S-state cycling of photosynthetic oxygen evolution. *J. Biol. Chem.* **280**, 2078–2083. (doi:10.1074/jbc.M410627200)

Lavorel, J. 1976 Matrix analysis of the oxygen evolving system of photosynthesis. *J. Theor. Biol.* **57**, 171–185. (doi:10.1016/S0022-5193(76)80011-2)

Loll, B., Kern, J., Saenger, W., Zouni, A. & Biesiadka, J. 2005 Towards complete cofactor arrangement in the 3.0 Å resolution structure of photosystem II. *Nature* **438**, 1040–1044. (doi:10.1038/nature04224)

Mäntele, W. 1996 Infrared and Fourier-transform infrared spectroscopy. In *Biophysical techniques in photosynthesis* (eds J. Amesz & A. J. Hoff), pp. 137–160. Dordrecht, The Netherlands: Kluwer Academic Publishers.

McEvoy, J. P. & Brudvig, G. W. 2006 Water-splitting chemistry of photosystem II. *Chem. Rev.* **106**, 4455–4483. (doi:10.1021/cr0204294)

McEvoy, J. P., Gascón, J. A., Batista, V. S. & Brudvig, G. W. 2005 The mechanism of photosynthetic water splitting. *Photobiochem. Photobiophys. Sci.* **4**, 940–949. (doi:10.1039/b506755c)

Meunier, P. C., Burnap, R. L. & Sherman, L. A. 1995 Modelling of the S-state mechanism and photosystem II manganese photoactivation in *Cyanobacteriae*. *Photosynth. Res.* **47**, 61–76. (doi:10.1007/BF00017754)

Mizusawa, N., Kimura, Y., Ishii, A., Yamanari, T., Nakazawa, S., Teramoto, H. & Ono, T.-A. 2004*a* Impact of replacement of D1 C-terminal alanine with glycine on structure and function of photosynthetic oxygen-evolving complex. *J. Biol. Chem.* **279**, 29 622–29 627. (doi:10.1074/jbc.M402397200)

Mizusawa, N., Yamanari, T., Kimura, Y., Ishii, A., Nakazawa, S. & Ono, T.-A. 2004*b* Changes in the functional and structural properties of the Mn cluster induced by replacing the side group of the C-terminus of the D1 protein of photosystem II. *Biochemistry* **43**, 14 644–14 652. (doi:10.1021/bi0486076)

Nakamoto, K. 1997 *Infrared and Raman spectra of inorganic and coordination compounds, Part b: applications in coordination, organometallic, and bioinorganic chemistry*, 5th edn. New York, NY: Wiley.

Nara, M., Torii, H. & Tasumi, M. 1996 Correlation between the vibrational frequencies of the carboxylate group and types of its coordination to a metal ion: an *ab Initio* molecular orbital study. *J. Phys. Chem.* **100**, 19 812–19 817. (doi:10.1021/jp9615924)

Noguchi, T. 2007 Light-induced FTIR difference spectroscopy as a powerful tool toward understanding the molecular mechanism of photosynthetic oxygen evolution. *Photosyn. Res.* **91**, 59–69. (doi:10.1007/s11120-007-9137-5)

Noguchi, T. In press. Fourier transform infrared analysis of the photosynthetic oxygen-evolving center. *Coord. Chem. Rev.*

Noguchi, T. & Berthomieu, C. 2005 Molecular analysis by vibrational spectroscopy. In *Photosystem II: the light-driven water:plastoquinone oxidoreductase* (eds T. Wydrzynski & Ki. Satoh), pp. 367–387. Dordrecht, The Netherlands: Springer.

Noguchi, T. & Sugiura, M. 2002 Flash-induced FTIR difference spectra of the water oxidizing complex in moderately hydrated photosystem II core films: effect of hydration extent on S-state transitions. *Biochemistry* **41**, 2322–2330. (doi:10.1021/bi011954k)

Noguchi, T. & Sugiura, M. 2003 Analysis of flash-induced FTIR difference spectra of the S-state cycle in the photosynthetic water-oxidizing complex by uniform ^{15}N and ^{13}C isotope labeling. *Biochemistry* **42**, 6035–6042. (doi:10.1021/bi0341612)

Noguchi, T., Ono, T.-A. & Inoue, Y. 1995 Direct detection of a carboxylate bridge between Mn and Ca^{2+} in the photosynthetic oxygen-evolving center by means of Fourier transform infrared spectroscopy. *Biochim. Biophys. Acta* **1228**, 189–200. (doi:10.1016/0005-2728(94)00171-Z)

Qian, M., Dao, L., Debus, R. J. & Burnap, R. L. 1999 Impact of mutations within the putative Ca^{2+}-binding lumenal interhelical a–b loop of the photosystem II D1 protein on the kinetics of photoactivation and H_2O-oxidation in *Synechocystis* sp, PCC 6803. *Biochemistry* **38**, 6070–6081. (doi:10.1021/bi982331i)

Rosenberg, C., Christian, J., Bricker, T. M. & Putnam-Evans, C. 1999 Site-directed mutagenesis of glutamate residues in the large extrinsic loop of the photosystem II protein CP 43 affects oxygen-evolving activity and PSII assembly. *Biochemistry* **38**, 15 994–16 000. (doi:10.1021/bi991326r)

Sauer, K. & Yachandra, V. K. 2004 The water-oxidation complex in photosynthesis. *Biochim. Biophys. Acta* **1655**, 140–148. (doi:10.1016/j.bbabio.2003.07.004)

Sauer, K., Yano, J. & Yachandra, V. K. 2005 X-ray spectroscopy of the Mn_4Ca cluster in the water-oxidation complex of photosystem II. *Photosyn. Res.* **85**, 73–86. (doi:10.1007/s11120-005-0638-9)

Sproviero, E. M., Gascón, J. A., McEvoy, J. P., Brudvig, G. W. & Batista, V. S. 2006 QM/MM Models of the O_2-evolving complex of photosystem II. *J. Chem. Theory Comput.* **2**, 1119–1134. (doi:10.1021/ct060018l)

Strickler, M. A., Walker, L. M., Hillier, W. & Debus, R. J. 2005 Evidence from biosynthetically incorporated strontium and FTIR difference spectroscopy that the C-terminus of the D1 polypeptide of photosystem II does not ligate calcium. *Biochemistry* **44**, 8571–8577. (doi:10.1021/bi050653y)

Strickler, M. A., Hillier, W. & Debus, R. J. 2006 No evidence from FTIR difference spectroscopy that glutamate-189 of the D1 polypeptide ligates a Mn ion that undergoes oxidation during the S_0 to S_1, S_1 to S_2, or S_2 to S_3 transitions in photosystem II. *Biochemistry* **45**, 8801–8811. (doi:10.1021/bi060583a)

Strickler, M. A., Walker, L. M., Hillier, W., Britt, R. D. & Debus, R. J. 2007 No evidence from FTIR difference spectroscopy that aspartate-342 of the D1 polypeptide ligates a Mn ion that undergoes oxidation during the S_0 to S_1, S_1 to S_2, or S_2 to S_3 transitions in photosystem II. *Biochemistry* **46**, 3151–3160. (doi:10.1021/bi062195e)

Suzuki, H., Taguchi, Y., Sugiura, M., Boussac, A. & Noguchi, T. 2006 Structural perturbations of the carboxylate ligands to the Mn cluster upon Ca^{2+}/Sr^{2+} exchange in the S-state cycle of photosynthetic oxygen evolution as studied by flash-induced FTIR difference spectroscopy. *Biochemistry* **45**, 13 454–13 464. (doi:10.1021/bi061232z)

Taguchi, Y. & Noguchi, T. 2007 Drastic changes in the ligand structure of the oxygen-evolving Mn cluster upon Ca^{2+} depletion as revealed by FTIR difference spectroscopy. *Biochim. Biophys. Acta* **1767**, 535–540. (doi:10.1016/j.bbabio.2006.11.002)

Tang, X.-S. & Diner, B. A. 1994 Biochemical and spectroscopic characterization of a new oxygen-evolving photosystem II core complex from the Cyanobacterium *Synechocystis* sp, PCC 6803. *Biochemistry* **33**, 4594–4603. (doi:10.1021/bi00181a021)

Yachandra, V. K. 2005 The catalytic manganese cluster: organization of the metal ions. In *Photosystem II: the light-driven water:plastoquinone oxidoreductase* (eds T. Wydrzynski & Ki. Satoh), pp. 235–260. Dordrecht, The Netherlands: Springer.

Yamanari, T., Kimura, Y., Mizusawa, N., Ishii, A. & Ono, T.-A. 2004 Mid- to low-frequency Fourier transform infrared spectra of S-state cycle for photosynthetic water oxidation in *Synechocystis* sp, PCC 6803. *Biochemistry* **43**, 7479–7490. (doi:10.1021/bi0362323)

Yano, J. *et al.* 2005 X-ray damage to the Mn_4Ca complex in single crystals of photosystem II: a case study for metalloprotein crystallography. *Proc. Natl Acad. Sci. USA* **102**, 12 047–12 052. (doi:10.1073/pnas.0505207102)

Yano, J. *et al.* 2006 Where water is oxidized to dioxygen: structure of the photosynthetic Mn_4Ca cluster. *Science* **314**, 821–825. (doi:10.1126/science.1128186)

Discussion

F. M. Ho (*Molecular Biomimetics, Department of Photochemistry and Molecular Science, Uppsala University, Uppsala, Sweden*). Regarding the ongoing debate about $S_2 \rightarrow S_3$ transition in the S-state cycle, if an oxidation step is ligand based rather than Mn based, what would you expect to be the nature and magnitude of changes in the S_{n+1}-*minus*-S_n FTIR difference spectrum due to the mutation of a ligand of a Mn ion close to the site of oxidation? Would this technique be diagnostic enough to distinguish between the ligand- and Mn-based oxidation scenarios?

R. J. Debus. FTIR difference spectroscopy should be able to detect either ligand- or Mn-based oxidation. However, before FTIR can be applied to distinguishing between the two oxidation scenarios during the $S_2 \rightarrow S_3$ transition, the residues whose vibrational modes are altered during this and other S-state transitions must be identified and the basis for the alteration of their modes must be understood.

I. Vass (*Institute of Plant Biology, Biological Research Centre, Szeged, Hungary*). I wish to comment. Modifications of the $S_2Q_A^-$ charge recombination characteristics in D1-H332 and CP43-E354 are very similar (fast $S_2Q_A^-$ and block of S-state transitions beyond S_2), which would support a model in which both D1-H332 and CP43-E354 ligate Mn2, instead of D1-H332 ligating Mn1.

R. J. Debus. I believe that inferences drawn from comparisons of mutants must be drawn with great care. For example, the CP43-E354Q mutant exhibits a normal quantum yield of S_2-state formation and a substantially unaltered S_2-state multiline EPR spectrum, whereas the D1-H332E mutant exhibits an extraordinarily low quantum yield of S_2-state formation and a substantially altered S_2-state multiline EPR signal. These differences might support a different model than that proposed by the questioner.

T. Noguchi (*Institute of Materials Science, University of Tsukuba, Tsukuba, Japan*). My comment is related to that of Dr Vass. Since a His band appears in the FTIR difference spectrum upon the $S_1 \rightarrow S_2$ transition, the His could be ligated to Mn2 that bears CP43-Glu354 as a ligand.

R. J. Debus. That is true. However, until D1-His332 mutants are investigated by FTIR, one cannot exclude the possibility that the His band in the S_2-*minus*-S_1 FTIR difference spectrum arises from D1-His337 or another histidine.

G. Brudvig (*Department of Chemistry, Yale University, Yale, USA*). My question relates to charge delocalization in the cluster when the oxidation steps occur and to the observation that many of the mutations show changes on $S_1 \rightarrow S_2$ which is the step when the Mn cluster increases its charge. Could the FTIR changes in $S_1 \rightarrow S_2$ reflect the charge build-up and be observed for many of the residues ligated and near to the Mn cluster, whereas the FTIR changes during the other S-state transitions for Mn ligands may not be detected because the charge is delocalized?

R. J. Debus. Most of the mutants that have been examined (D1-Asp170His, D1-Glu189Gln, D1-Glu189Arg, D1-Asp342Asn) produce no appreciable alterations in any of the S_{n+1}-*minus*-S_n FTIR difference

spectra. The lack of alterations implies either that the charge that is produced during the $S_1 \rightarrow S_2$ transition is localized to the Mn ion that is ligated by D1-Ala344 or that the charge is sufficiently delocalized that most residues are insensitive to its formation. The downshift of the symmetric carboxylate stretching mode of D1-Ala344 during the $S_1 \rightarrow S_2$ transition may be caused by something other than the increased charge on the cluster, as you have suggested previously.

F. Manedov (*Molecular Biomimetics, Department of Photochemistry and Molecular Science, Uppsala University, Uppsala, Sweden*). In some mutants used in this study, part of the PSII centres lack the Mn cluster. Could these Mn-depleted centres contribute to the FTIR difference spectra and to what extent?

R. J. Debus. It is true that, in many mutants, a significant fraction of PSII centres lack the Mn cluster. In some of these mutants, the presence of Mn-depleted centres causes the S_2-*minus*-S_1 FTIR difference spectrum to contain contributions from $Y_Z^{\cdot} - Y_Z$ or $Y_D^{\cdot} - Y_D$ depending on temperature and illumination conditions. However, these contributions can be identified and removed by a relatively simple subtraction procedure. The S_2-*minus*-S_1 FTIR difference spectrum of the CP43-Glu354Gln mutant appears to contain no contribution from either tyrosyl radicals.

H. Dau (*FB Physik, Freie University, Berlin, Germany*). For several mutations of putative Mn ligands, you have observed, when comparing wild-type and mutant PSII, only small changes in the FTIR difference spectra of the four transitions between semi-stable S states; these changes were of similar magnitude as changes caused by different buffer conditions (Strickler *et al.* 2007). Therefore, you have proposed that secondary structural perturbations unrelated to amino acid ligands of the Mn complex may give rise to such small-amplitude contributions to the FTIR difference spectra. Can you suggest an explanation why the bands related to, for example, remote carboxylate are all of smaller amplitude than the bands which are assignable to carboxylates of the Mn–ligand environment?

R. J. Debus. A mutation-induced shift of a vibrational mode should have the same appearance in a specific S_{n+1}-*minus*-S_n FTIR difference spectrum irrespective of the mutated residue's distance from the Mn_4Ca cluster. Our point is that great care must be taken in interpreting small changes in the FTIR difference spectra of proteins that contain site-directed mutations. Any site-directed mutation in PSII will introduce a myriad of subtle changes to hydrogen bonds, peptide bond conformations and long-range electrostatic interactions, irrespective of whether the mutated residue ligates the Mn_4Ca cluster or not. These small structural perturbations can be transmitted to residues whose vibrational modes change during specific S-state transitions, causing subtle changes to the absolute absorption spectra of these residues. Such subtle changes to absolute absorption spectra would likely give rise to small changes in S_{n+1}-*minus*-S_n FTIR difference spectra. In contrast, a mutation-induced *elimination* of a vibrational mode that shifts during an S-state transition should be as obvious in a difference spectrum as the [$1-^{13}$C]alanine-induced shift of the $\nu_{sym}(COO^-)$ mode of D1-Ala344.